common in animals (for example, see ref. 17); the lack of functional transfer may reflect a stringent barrier imposed by genetic code incompatibilities in animals but not plants. Multiple, probably mostly ancient, losses have been inferred for many mitochondrial and chloroplast genes across the broad sweep of eukaryotic evolution[18–20]. However, corresponding nuclear genes have generally been isolated from at most a single loss lineage, and therefore the incidence of (parallel) gene transfer is unclear.

The high rates of *rps10* loss and transfer in angiosperms seem to equal or exceed rates of two much simpler and, one would think, much more likely classes of mitochondrial mutations in angiosperms. These include intron loss (Fig. 1; our own unpublished data) and perhaps even the trivial mutation of substitution at a silent site in a protein gene. This is surprising, considering that functional gene transfer is such a complex, multistep process, involving reverse transcription of a mitochondrial messenger RNA, movement to the nucleus, chromosomal integration, gain of a nuclear promoter and other regulatory elements, gain of a presequence (usually), and, ultimately, mitochondrial gene loss. Relocation of *rps10* to the nucleus is occurring at a dizzying pace in angiosperms, with the many cases showing a remarkable range of opportunistic gene fusions and co-options leading to functional activation with or without gain of a mitochondrial presequence. □

Methods

Total cellular DNA and RNA were isolated as described[3]. For Southern blot hybridization, total genomic DNAs were cut with *Hin*dIII, electrophoresed, blotted and hybridized[3] at moderate stringency (60 °C in 5 × SSC; washes at 60 °C in 2 × SSC). We isolated nuclear (16) and mitochondrial (30) *rps10* genes by PCR, reverse transcription-PCR and 5′ rapid amplification of cDNA ends as described[3] (see Supplementary Information for primers and inverse PCR). All PCR products were sequenced directly, or cloned using the TA cloning kit (Invitrogen) followed by sequencing of multiple clones. Maximum likelihood analyses were conducted using PAUP*4.0b3a (ref. 21). We used the HKY85 model, assuming a discrete gamma distribution with four categories of site-to-site rate variability. For each analysis, we estimated the transition/transversion ratio and base frequencies using Tree-PUZZLE (version 4.02 (ref. 22)) under the HKY model of evolution, with gamma-distributed rates and parameter estimation set to 'approximate'. We excluded the five RNA editing sites. Our analyses used heuristic searches with random-taxon addition (10 replicates) and TBR branch-swapping. We carried out all analyses at least twice until a stable topology was achieved. Bootstrapping was done using PAUP* as above, with stepwise addition and 100 replicates.

The mitochondria from soybean cotyledons[23] and potato tubers[24] were prepared. ^{35}S-labelled RPS10 precursor proteins were synthesized from cDNA clones and imported into the isolated mitochondria *in vitro*[25]. In some cases, smaller precursor proteins were denatured before import[26].

Received 11 May; accepted 16 August 2000.

1. Gray, M. W. The endosymbiont hypothesis revisited. *Int. Rev. Cytol.* **141,** 233–357 (1992).
2. Boore, J. L. Animal mitochondrial genomes. *Nucleic Acids Res.* **27,** 1767–1780 (1999).
3. Adams, K. L. *et al.* Intracellular gene transfer in action: Dual transcription and multiple silencings of nuclear and mitochondrial *cox2* genes in legumes. *Proc. Natl Acad. Sci. USA* **96,** 13863–13868 (1999).
4. Wolfe, K. H., Li, W. -H. & Sharp, P. M. Rates of nucleotide substitution vary greatly among plant mitochondrial, chloroplast, and nuclear DNAs. *Proc. Natl Acad. Sci. USA* **84,** 9054–9058 (1987).
5. Laroche, J., Li, P., Maggia, L. & Bousquet, J. Molecular evolution of angiosperm mitochondrial exons and introns. *Proc. Natl Acad. Sci. USA* **94,** 5722–5727 (1997).
6. Kadowaki, K., Kubo, N., Ozawa, K. & Hirai, A. Targeting presequence acquisition after mitochondrial gene transfer to the nucleus occurs by duplication of existing targeting signals. *EMBO J.* **15,** 6652–6661 (1996).
7. Figueroa, P., Gómez, I., Holuigue, L., Araya, A. & Jordana, X. Transfer of *rps14* from the mitochondrion to the nucleus in maize implied integration within a gene encoding the iron-sulphur subunit of succinate dehydrogenase and expression by alternative splicing. *Plant J.* **18,** 601–609 (1999).
8. Kubo, N., Harada, K., Hirai, A. & Kadowaki, K. A single nuclear transcript encoding mitochondrial RPS14 and SDHB of rice is processed by alternative splicing: Common use of the same mitochondrial targeting signal for different proteins. *Proc. Natl Acad. Sci. USA* **96,** 9207–9211 (1999).
9. Wischmann, C. & Schuster, W. Transfer of *rps10* from the mitochondrion to the nucleus in *Arabidopsis thaliana*: evidence for RNA-mediated transfer and exon shuffling at the integration site. *FEBS Lett.* **375,** 152–156 (1995).
10. Kubo, N. *et al.* Transfer of the mitochondrial *rps10* gene to the nucleus in rice: acquisition of the 5′ untranslated region followed by gene duplication. *Mol. Gen. Genet.* **263,** 733–739 (2000).
11. Nakagawa, T., Maeshima, M., Nakamura, K. & Asahi, T. Molecular cloning of a cDNA for the smallest nuclear-encoded subunit of sweet potato cytochrome *c* oxidase. *Eur. J. Biochem.* **191,** 557–561 (1990).
12. Morikami, A., Ehara, G. & Yuuki, K. Molecular cloning and characterization of cDNAs for the γ-subunit and ϵ-subunit of mitochondrial F1F0 ATP synthase from sweet potato. *J. Biol. Chem.* **268,** 17205–17210 (1993).
13. Braun, H.-P., Jansch, L., Kruft, V. & Schmitz, U. K. The 'Hinge' protein of cytochrome c reductase from potato lacks the acidic domain and has no cleavable presequence. *FEBS Lett.* **347,** 90–94 (1994).
14. Long, M., de Souza, S. J., Rosenberg, C. & Gilbert, W. Exon shuffling and the origin of the mitochondrial targeting function in plant cytochrome c1 precursor. *Proc. Natl Acad. Sci. USA* **93,** 7727–7731 (1996).
15. Herrmann, R. G. in *Eukaryotism and Symbiosis* (eds Schenk, H. E. A. *et al.*) 73–118 (Springer, Vienna, 1997).
16. Figueroa, P. *et al.* The gene for mitochondrial ribosomal protein S14 has been transferred to the nucleus in *Arabidopsis thaliana*. *Mol. Gen. Genet.* **262,** 139–144 (1999).
17. Bensasson, D., Zhang, D.-X. & Hewitt, G. M. Frequent assimilation of mitochondrial DNA by grasshopper nuclear genomes. *Mol. Biol. Evol.* **17,** 406–415 (2000).
18. Palmer, J. D. The mitochondrion that time forgot. *Science* **275,** 790–791 (1997).
19. Martin, W. *et al.* Gene transfer to the nucleus and the evolution of chloroplasts. *Nature* **393,** 162–165 (1998).
20. Gray, M. W. Evolution of organellar genomes. *Curr. Opin. Genet. Dev.* **9,** 678–687 (1999).
21. Swofford, D. L. PAUP*, *Phylogenetic Analysis Using Parsimony (*and Other Methods)* 4.0B3 edn (Sinauer Associates, Sunderland, MA, 2000).
22. Strimmer, K. & von Haeseler, A. Quartet puzzling: A quartet maximum likelihood method for reconstructing tree topologies. *Mol. Biol. Evol.* **13,** 964–969 (1996).
23. Day, D. A., Neuburger, M. & Douce, R. Biochemical characterization of chlorophyll-free mitochondria from pea leaves. *Aust. J. Plant Phys.* **12,** 219–228 (1985).
24. Neuberger, M., Journet, E., Bligny, R., Carde, J. & Douce, R. Purification of plant mitochondria by isopycnic centrifugation in density gradients of percoll. *Arch. Biochem. Biophys.* **217,** 312–323 (1982).
25. Tanudji, M., Sjoling, S., Glaser, E. & Whelan, J. Signals required for the import and processing of the alternative oxidase into mitochondria. *J. Biol. Chem.* **274,** 1286–1293 (1999).
26. Knox, C., Sass, E., Neupert, W. & Pines, O. Import into mitochondria, folding, and retrograde movement of fumarase in yeast. *J. Biol. Chem.* **273,** 25587–25593 (1998).
27. Soltis, P. S., Soltis, D. E. & Chase, M. W. Angiosperm phylogeny inferred from multiple genes as a tool for comparative biology. *Nature* **402,** 402–404 (1999).

Supplementary information is available on *Nature*'s World-Wide Web site (http://www.nature.com) or as paper copy from the London editorial office of *Nature*.

Acknowledgements

We thank W. Fischer, J. Logsdon, C. Parkinson, M. Rosenblueth, N. Schisler and K. Wolfe for reading the manuscript, and D. Swofford for allowing us to use a pre-release version of PAUP*. This study was supported by a United States Department of Agriculture graduate fellowship to K.L.A., grants to Y.L.Q. and J.D.P. from the NIH, and grants from the Australian Research Council to J.W.

Correspondence and requests for materials should be addressed to J.D.P. (e-mail: jpalmer@bio.indiana.edu). The sequences reported in this study have been deposited in GenBank under the accession numbers AF287307–AF287345.

Imagery neurons in the human brain

Gabriel Kreiman*, Christof Koch* & Itzhak Fried†

* *Computation and Neural Systems Program, California Institute of Technology, 139-74, Pasadena, California 91125, USA*
† *Division of Neurosurgery, and Department of Psychiatry and Biobehavioral Sciences, University of California at Los Angeles, School of Medicine, 740 Westwood Plaza, Los Angeles, California 90095, USA*

Vivid visual images can be voluntarily generated in our minds in the absence of simultaneous visual input. While trying to count the number of flowers in Van Gogh's *Sunflowers*, understanding a description or recalling a path, subjects report forming an image in their "mind's eye"[1]. Whether this process is accomplished by the same neuronal mechanisms as visual perception has long been a matter of debate[1–3]. Evidence from functional imaging[1,4–8], psychophysics[1,9], neurological studies[2] and monkey electrophysiology[10–12] suggests a common process, yet there are patients with deficits in one but not the other[3,13]. Here we directly investigated the neuronal substrates of visual recall by recording from single neurons in the human medial temporal lobe[14,15] while the subjects were asked to imagine previously viewed images. We found single neurons in the hippocampus, amygdala, entorhinal cortex and parahippocampal gyrus that selectively altered their firing rates depending on the stimulus the subjects were imagining. Of the neurons that fired selectively during both vision and imagery, the majority (88%) had identical selectivity. Our study reveals single neuron correlates of volitional visual imagery in humans and

suggests a common substrate for the processing of incoming visual information and visual recall.

We directly studied the neuronal correlates of visual imagery by recording from single neurons in the human brain. Subjects were nine patients with pharmacologically intractable epilepsy implanted with chronic electrodes to localize the seizure foci for possible surgical resection[14]. Based on clinical criteria, electrodes were implanted bilaterally in the amygdala, entorhinal cortex, hippocampus and parahippocampal gyrus. We compared the selectivity of the neurons during vision and visual imagery for different stimuli. Two images were separately shown for 1,000 ms per presentation and five repetitions per image (Fig. 1a, b). Figures were drawn from the following nine groups: faces showing emotions, household objects, spatial layouts, cars, animals, drawings and photographs of famous people, foodstuffs and complex patterns[15]. Subsequently, the subjects closed their eyes and imagined one of the two pictures shown upon listening to a high or low tone (Fig. 1d). Tones were alternated every 3,000 ms and there were five repetitions of the tones per image. Visual imagery was verified by debriefing after each pair of pictures.

We recorded from 276 single neurons in the medial temporal lobe (Table 1). We found that some of the neurons showed selective changes in firing rate while subjects viewed the figures and when they were visually recalling the images with closed eyes. A neuron was considered to be selective to one of the stimulus groups if: (1) the firing rate during stimulus presentation was significantly different from the baseline activity (Wilcoxon test); (2) the response was different from that to stimuli from all other stimulus groups (analysis of variance (ANOVA) and pairwise Wilcoxon comparisons); and (3) no significant differences were found in the response to distinct individual stimuli within the group (ANOVA).

The baseline activity of the neurons during vision was computed in the 1,000-ms interval before each presentation. During visual imagery, we avoided comparing to a baseline between tones when subjects could still be imagining the stimuli; instead, we used the 1,000-ms interval before the first tone. Neuronal activity during the baseline constitutes a potential concern in visual imagery experiments[1,5,7]. There was no significant difference in the firing rate of any of the neurons in the vision and imagery baselines (Wilcoxon test, $P > 0.2$). Furthermore, both baselines were indistinguishable from the spontaneous activity of the neurons computed over the entire experimental session.

Figure 2a shows an example of activity recorded from a neuron in the entorhinal cortex that increased its firing rate selectively when the subject viewed pictures of objects. The mean firing rate during the interval between 100 and 1,000 ms after stimulus onset for objects was 16.8 ± 3.6 (mean ± s.d.) spikes per second. This was significantly higher than the baseline and also higher than the activity for all other types of stimulus (ANOVA and pairwise comparisons, $P < 10^{-3}$). The same neuron also increased its firing rate when the patient recalled the objects with closed eyes (Fig. 2b), but not when the subject imagined other stimuli. Activity recorded from another example of a neuron that showed selective changes in firing rate during vision and visual recall is shown in Fig. 3. This

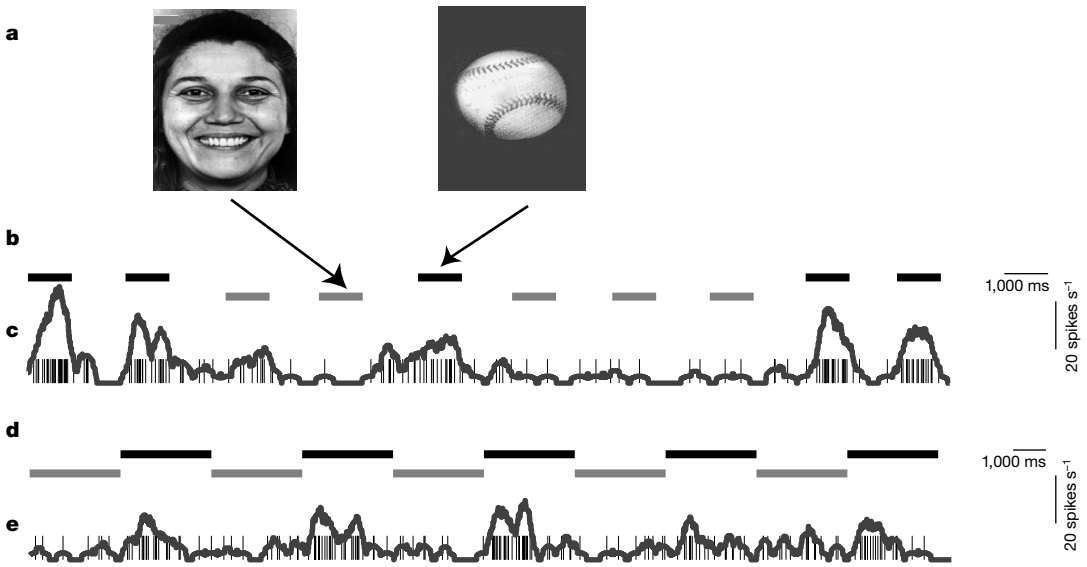

Figure 1 Individual responses of a single neuron during vision and imagery. **a,** Two images were shown separately for 1,000 ms each, five repetitions per image, indicated by horizontal black and white bars in **b**. After each picture, subjects pressed a button indicating whether the picture was a human face. **c**, Activity from a neuron in the entorhinal cortex; the continuous line shows the spike density function. After 10 visual presentations, subjects closed their eyes and imagined one or the other picture upon hearing a high or low tone. **d**, Tones were alternated every 3,000 ms. **e**, Data from the same neuron during visual imagery. This neuron showed an increased firing rate for pictures of objects ($P < 10^{-3}$) during both vision and imagery.

Table 1 Number of responsive and selective neurons

	Amygdala	Entorhinal cortex	Hippocampus	Parahippocampal gyrus	Total
n	89	78	91	18	276
Visual responsive	12 (13%)	16 (21%)	17 (19%)	4 (22%)	49 (18%)
Visual selective	9 (10%)	14 (18%)	17 (19%)	4 (22%)	44 (16%)
Imagery responsive	8 (9%)	11 (14%)	9 (10%)	5 (28%)	33 (12%)
Imagery selective	4 (4%)	8 (10%)	8 (9%)	3 (17%)	23 (8%)
Both selective	3 (75%)	6 (75%)	5 (63%)	2 (67%)	16 (70%)

Number of responsive and selective neurons detected out of the number of neurons recorded in each location (*n*). The percentages for the responsive and selective neurons are based on the total number of recorded neurons. 'Both selective' indicates those neurons selective during vision and imagery. For these, the percentages are based on the total number of imagery selective neurons. Of the 16 neurons selective during both processes, 14 showed the same selectivity. The neurons were selective for faces, objects, spatial layouts and other stimuli. A χ^2 test[14] to address the probability of obtaining the number of selective neurons by chance yielded $P < 0.01$ for the 28 vision-only neurons, $P = 0.04$ for the 7 imagery-only neurons and $P < 10^{-5}$ for the 16 neurons selective during both.

amygdala neuron (from a different patient) showed an increased firing rate when the subject saw pictures of animals and when she formed mental images of the same pictures, but not during vision or recall of other stimuli.

We found a total of 44 neurons (16% of all recorded neurons) that showed selective changes in firing rate during visual presentation (Table 1). There were 23 neurons (8%) that showed selective changes in firing rate while subjects visually imagined the same stimuli. Of these 23 neurons, 7 (30%) were activated exclusively during imagery whereas 16 (70%) were selective during vision. Remarkably, of these 16 neurons, 14 (88%) showed the same selectivity during vision and visual imagery. While the significance criterion was set to 0.05, most of the *P* values (vision: 78%; imagery: 67%) were below 0.01. Assuming a null hypothesis of independence between vision and imagery, at the 0.01 level we would expect approximately one neuron in 90,000 to show the same selectivity during both vision and imagery by chance. We found 10 neurons in our sample of 276 neurons with $P < 0.01$ (and 14 with $P < 0.05$) that responded with the same selectivity during vision and imagery. As is consistent with the longer period of the imagery task and the more temporally diffuse nature of imagery, the latencies and the time of peak activity were longer and more variable for imagery than for vision (latency was 282 ± 191 ms for vision and 409 ± 291 ms for imagery; peak time was 665 ± 247 ms for vision and 1,482 ± 921 ms for imagery).

Does the firing rate of the neurons during vision differ during imagery of the same stimuli? To address this question, for the 14 neurons with the same selectivity we computed the firing rate over the whole stimulus period for the selective stimuli and divided it by the baseline activity. There was a strong correlation between this normalized firing response for vision and visual imagery ($r^2 = 0.90$). The slope between the activity during vision and imagery was 0.74, indicating that the firing rates were about 25% higher during vision. As the duration of the selective response was typically shorter than

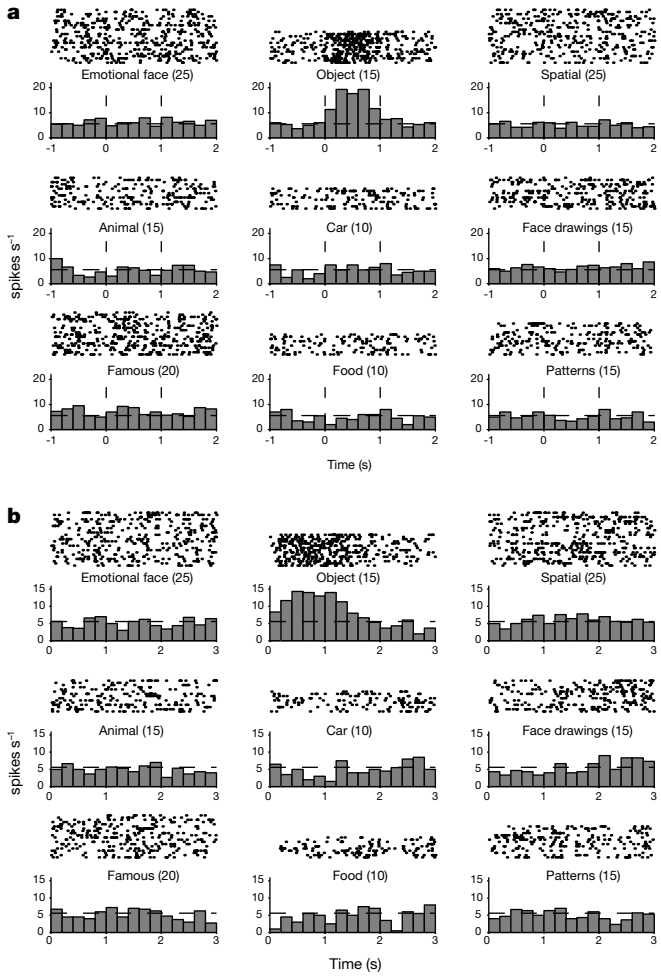

Figure 2 Responses of the same neuron as in Fig. 1 during vision and visual imagery. **a**, During vision; **b**, during visual imagery. The post-stimulus time histograms were computed by averaging activity for all stimuli within each stimulus group (the total number of presentations is indicated in parentheses) using a bin size of 200 ms. This neuron increased its firing rate over the baseline ($P < 10^{-4}$) upon visually presenting objects but not other stimuli. An ANOVA and pairwise comparisons indicated that the response to objects was significantly different from that to other stimuli ($P < 10^{-3}$). The neuron also increased its activity when the subject recalled the same objects in her mind with eyes closed (comparison with baseline, ANOVA and pairwise comparisons: $P < 0.001$) but not during imagery of other stimuli. There was no significant difference in the responses to distinct objects (vision $P > 0.2$; imagery $P > 0.2$).

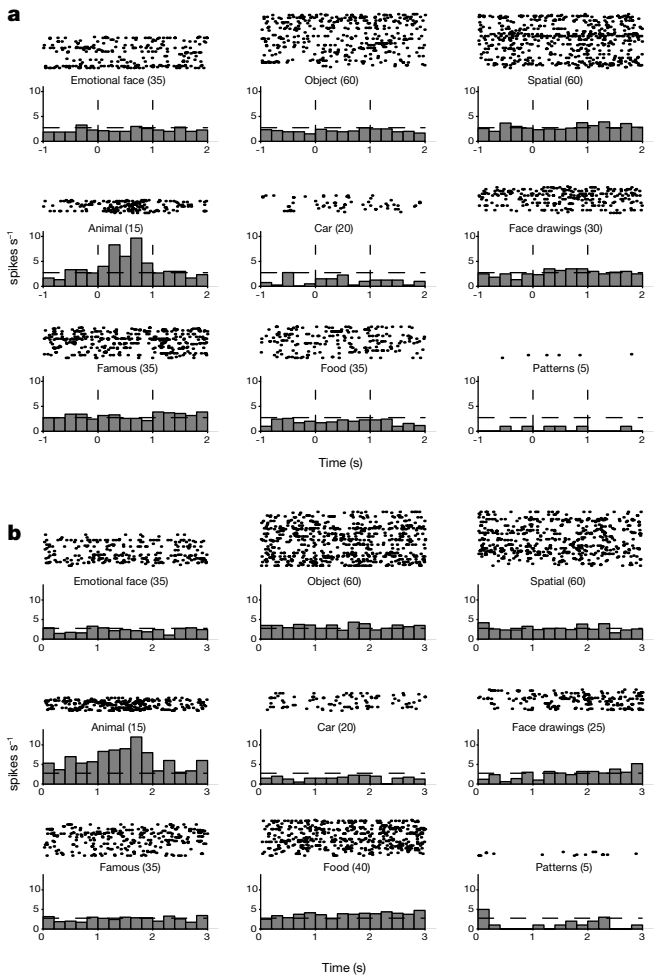

Figure 3 Responses of a selective neuron in the left amygdala of a different subject during vision and visual imagery. **a**, During vision; **b**, during visual imagery. This neuron increased its firing rate over the baseline upon visually presenting animals ($P < 10^{-5}$) and also during imagery of animals ($P < 10^{-4}$) but not to other stimuli. ANOVA and pairwise comparisons also showed that the response of this neuron was highly selective during both vision ($P < 10^{-3}$) and visual imagery ($P < 10^{-3}$). There was no significant difference in the responses to distinct animals (vision $P > 0.15$; imagery $P > 0.3$).

the whole stimulus period (mean 560 ± 292 ms for vision and 948 ± 580 ms for imagery), this firing rate is an underestimation of the response of the neuron. Furthermore, the intervals in the two tasks were different. We therefore computed the firing rates in a 600-ms period centred on the peak firing rate. The correlation coefficient between the firing rate in this interval during vision and imagery was 0.95 and the slope was 0.85 (Fig. 4a). Given the weaker percept during imagery, it may seem surprising that the difference in firing responses is so small. Yet, in our sample there were fewer cells recruited during visual imagery than during vision (Table 1). Similar results were observed by functional imaging studies[7]. Selectivity to one of the categories may be due to physical similarity between the stimuli. The correlation of firing rates between vision and imagery was also high for individual figures ($r^2 = 0.93$, slope is 0.88; see for example Fig. 1.) Therefore, the correlation does not rely on category selectivity. Furthermore, there was no significant difference between the responses to distinct individual stimuli within the selective group for the selective neurons (ANOVA, vision $P > 0.1$; imagery $P > 0.15$.)

Is it possible for an ideal observer to predict the group of the stimulus that the subject was viewing or imagining on the basis of the firing rate of a single neuron? Figure 1 shows a particularly clear example of selective firing in a single repetition of the neuron whose average activity was depicted in Fig. 2. By observing the activity of this neuron, it is possible to predict with rather high accuracy what the subject was viewing (Fig. 1c) or imagining (Fig. 1e). We addressed this question quantitatively by carrying out a receiver operating characteristic analysis[16]. This yielded the minimum probability of error, P_e, in classifying the stimulus as belonging to the preferred category or not on the basis of the average firing rate[15]. $P_e = 0$ corresponds to perfect classification and $P_e = 0.5$ to chance performance. P_e ranged from 0.10 to 0.44 for vision (0.28 ± 0.07) and from 0.08 to 0.46 for visual imagery (0.27 ± 0.06). There was a strong correlation in the P_e values for the neurons selective in both vision and imagery (Fig. 4b).

Extrastriate areas in the human brain are specialized for processing complex visual input. For instance, functional magnetic resonance imaging studies show areas specialized for faces[17] and places[18]. Neurons in monkey extrastriate cortex respond selectively to complex stimuli[19–22]. Their activity represents the pictorial short-term memory[11,23,24] and neuronal correlates of visual recall and prospective coding have been described in monkeys[10–12]. Furthermore, these studies show top-down interactions between prefrontal and temporal cortex during recall. These neurons project to the medial temporal lobe[20,25] where lesions lead to specific visual deficits in both macaques and humans[2,17,19,20,26,27]. Furthermore, electrical stimulation in the human temporal lobe can interfere with[28,29] or elicit visual recall[30].

We observed three different types of selective neurons. Some neurons responded during processing of incoming visual information but not during imagery (28/44). There were also neurons activated only during visual recall (7/23), which may be involved in retrieval mechanisms dissociated from vision[3,13]. Finally, some neurons responded selectively during both vision and imagery (16/23). Of these 16 neurons, 14 showed identical selectivity. There are patients with deficits in both vision and imagery[1,2], but some neurological lesions yield impairments in one but not the other[3,13]. There is considerable convergence of input to the medial temporal lobe and it is plausible that these lesions involve neuronal systems that project to neurons in the areas studied here. We did not find regional segregation of neurons selective during vision and imagery; both were found in all regions (Table 1). Although our data suggest shared neuronal representation in the medial temporal lobe, it does not rule out the possibility of segregation between these processes.

Our results provide a rare opportunity to observe the activity of single neurons in the human brain directly in the absence of external visual stimulation. This activity may represent the retrieval of the picture information from memory or the maintenance of the visual percept during imagination. The firing of these neurons could represent a correlate of the percept common to vision and imagery. Given the prominent role of the medial temporal lobe in declarative memory, it also seems possible that these neurons could be activated during storage of incoming visual inputs and later reactivated during the mnemonic retrieval process required for imagery. □

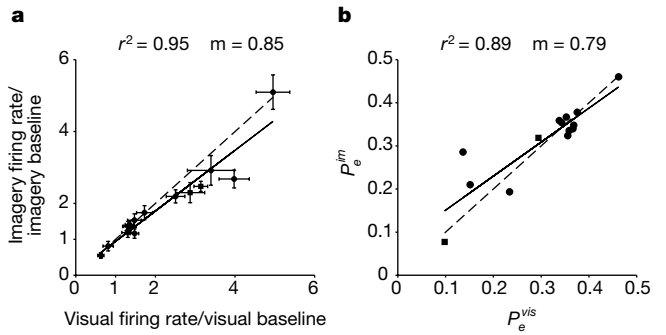

Figure 4 Comparison of firing rates and P_e between vision and imagery. **a**, Correlation of firing rates between vision and visual imagery for the 14 neurons that showed the same selectivity (Table 1). The firing rate was computed in a 600-ms window centred on the response peak and normalized by the baseline. The dashed line indicates $y = x$. The solid line shows a linear fit (slope is 0.85; correlation coefficient is 0.95; r^2 between the absolute firing rates is 0.93 and r^2 between the firing rates after subtracting the baseline is 0.97). The error bars correspond to standard deviation. **b**, Probability of error (P_e) in predicting the visual or the imagined percept on the basis of the firing rate of a single neuron. The P_e ranges from 0 (perfect classification) to 0.5 (chance performance). The dashed line shows $y = x$. The solid line indicates the linear fit (slope is 0.79; $r^2 = 0.89$). The examples from the previous figures are indicated by squares.

Methods

Subjects and electrode implantation

Subjects were nine patients (21–42 years old, four male, seven right-handed) with pharmacologically intractable epilepsy. Extensive non-invasive monitoring did not yield concordant data corresponding to a single resectable focus and, therefore, they were implanted with chronic depth electrodes for 1–2 weeks to determine the seizure focus for possible surgical resection[14,15]. The surgeries were performed by I.F. All studies conformed with the guidelines of the Medical Institutional Review Board at UCLA. Four of the patients also participated in a previous study where only visual responses were examined[15]. The location of the electrodes was verified by structural magnetic resonance imaging. The electrode locations were based exclusively on clinical criteria. The recordings during seizures were used to localize the focus. We note that generalization about normal neuronal function from recordings in epileptic patients constitutes a potential limitation. However, 87% of the recorded neurons were outside the clinically determined epileptogenic zone and we did not observe differences in waveforms or response properties in neurons near the seizure focus.

Tasks and recordings

During vision, two images were separately shown for 1,000 ms (Fig. 1a and b). In the first two patients, only faces, objects and spatial layouts were presented. After each picture, a tone reminded the subjects to press a button indicating whether the picture was a human face. Subsequently, subjects closed their eyes and imagined one or the other picture upon listening to high and low tones alternated every 3,000 ms (Fig. 1d). This was repeated for approximately 30 different pairs of images during each session, 2–4 sessions per patient, depending on clinical constraints. Imagery was verified by debriefing following each repetition by requesting detailed descriptions and asking whether subjects could form visual images. Each image appeared in only one pair. Three neurons (none selective) showed a different activity to high and low tones per se. We compared the activity before and after the behavioural response and the peri-response activity to the baseline. None of the visual or imagery neurons showed firing related to pressing the button. We also observed selectivity previously without behavioural responses[14].

Data from each recorded microwire were amplified, high-pass filtered and stored for off-line cluster separation (Datawave). Because the microelectrodes were chronically implanted, no selection of neurons by moving the electrodes was performed. Typically, neurons recorded from the same microwire as a selective neuron were not selective. We did not find evidence of spatial segregation of selective responses within any region. Because the location of the electrodes was fixed and based on clinical criteria, we were not able to address what happens in lower visual areas.

Data analysis

A neuron was considered selective to a stimulus group if: (1) the firing rate during stimulus presentation was different from the preceding baseline (Wilcoxon test, < 0.05), (2) an analysis of variance and pairwise comparisons (Wilcoxon test) addressing whether there were differences among the stimulus groups yielded $P < 0.05$ and (3) an ANOVA (parametric and non-parametric) comparing the variability to distinct stimuli within the selective category to the variability to repeated presentations of the same stimulus showed $P>0.05$. We observed neurons selective to faces, objects, spatial layouts and other stimuli.

If the across-groups comparisons were not significant but the activity was different from baseline, the neuron was defined as responsive but non-selective. To take into account any effects due to the different intervals we also compared the responses in a 600-ms window centred on the peak firing rate. The peak, latency and duration were estimated from the spike density function[15]. For the selective neurons we computed the probability of error, P_e, for classifying the stimulus as belonging to the preferred stimulus category or not[15,16]. We did not observe any difference between the right and left hemisphere neurons.

Received 21 July; accepted 22 August 2000.

1. Kosslyn, S. M. *Image and Brain* (MIT Press, Cambridge, 1994).
2. Farah, M. J. Is visual imagery really visual? Overlooked evidence from neuropsychology. *Psychol. Rev.* **95,** 307–317 (1988).
3. Behrmann, M., Winocur, G. & Moscovitch, M. Dissociation between mental imagery and object recognition in a brain-damaged patient. *Nature* **359,** 636–637 (1992).
4. Kosslyn, S. M., Thompson, W. L. & Alpert, N. M. Neural systems shared by visual imagery and visual perception: a PET study. *Neuroimage* **6,** 320–334 (1997).
5. Roland, P. E. & Gulyas, B. Visual imagery and visual representation. *Trends Neurosci.* **17,** 281–287 (1994).
6. D'Esposito, M. *et al.* A fMRI study of mental image generation. *Neuropsychologia* **35,** 725–730 (1997).
7. O'Craven, K. & Kanwisher, N. Mental imagery of faces and places activates corresponding stimulus-specific brain regions. *J. Cog. Neurosci.* (in the press).
8. Frith, C. & Dolan, R. J. Brain mechanisms associated with top-down processes in perception. *Phil. Trans. R. Soc. Lond.* **352,** 1221–1230 (1997).
9. Ishai, A. & Sagi, D. Common mechanisms of visual imagery and perception. *Science* **268,** 1772–1774 (1995).
10. Rainer, G., Rao, S. & Miller, E. Prospective coding for objects in primate prefrontal cortex. *J. Neurosci.* **19,** 5493–5505 (1999).
11. Miyashita, Y. & Chang, H. S. Neuronal correlate of pictorial short-term memory in the primate temporal cortex. *Nature* **331,** 68–71 (1988).
12. Tomita, H., Ohbayashi, M., Nakahara, K., Hasegawa, I. & Miyashita, Y. Top-down signal from prefrontal cortex in executive control of memory retrieval. *Nature* **401,** 699–703 (1999).
13. Bartolomeo, P. *et al.* Multiple-domain dissociation between impaired visual perception and preserved mental imagery in a patient with bilateral extrastriate lesions. *Neuropsychologia* **36,** 239–249 (1998).
14. Fried, I., MacDonald, K. A. & Wilson, C. Single neuron activity in human hippocampus and amygdala during recognition of faces and objects. *Neuron* **18,** 753–765 (1997).
15. Kreiman, G., Koch, C. & Fried, I. Category-specific visual responses of single neurons in the human medial temporal lobe. *Nature Neurosci.* **3,** 946–953 (2000).
16. Green, D. & Swets, J. *Signal detection theory and psychophysics* (Wiley, New York, 1966).
17. Kanwisher, N. & Moscovitch, M. The cognitive neuroscience of face processing: An introduction. *Cogn. Neuropsychol.* **17,** 1–11 (2000).
18. Epstein, R. & Kanwisher, N. A cortical representation of the local visual environment. *Nature* **392,** 598–601 (1998).
19. Logothetis, N. K. & Sheinberg, D. L. Visual object recognition. *Annu. Rev. Neurosci.* **19,** 577–621 (1996).
20. Tanaka, K. Inferotemporal cortex and object vision. *Annu. Rev. Neurosci.* **19,** 109–139 (1996).
21. Gross, C. G. How inferior temporal cortex became a visual area. *Cereb. Cortex* **5,** 455–469 (1994).
22. Rolls, E. Neural organization of higher visual functions. *Curr. Opin. Neurobiol.* **1,** 274–278 (1991).
23. Miyashita, Y. Inferior temporal cortex: Where visual perception meets memory. *Annu. Rev. Neurosci.* **16,** 245–263 (1993).
24. Chelazzi, L., Duncan, J., Miller, E. K. & Desimone, R. Responses of neurons in inferior temporal cortex during memory-guided visual search. *J. Neurophys.* **80,** 2918–2940 (1998).
25. Suzuki, W. A. Neuroanatomy of the monkey entorhinal, perirhinal and parahippocampal cortices: Organization of cortical inputs and interconnections with amygdala and striatum. *Semin. Neurosci.* **8,** 3–12 (1996).
26. Warrington, E. & McCarthy, R. Categories of knowledge—Further fractionations and an attempted integration. *Brain* **110,** 1273–1296 (1987).
27. Meunier, M., Hadfield, W., Bachevalier, J. & Murray, E. Effects of rhinal cortex lesions combined with hippocampectomy on visual recognition memory in rhesus monkeys. *J. Neurophysiol.* **75,** 1190–1205 (1996).
28. Fried, I., Mateer, C., Ojemann, G., Wohns, R. & Fedio, P. Organization of visuospatial functions in human cortex. *Brain* **105,** 349–371 (1982).
29. Ojemann, G. & Mateer, C. Human language cortex: localization of memory, syntax, and sequential motor-phoneme identification systems. *Science* **205,** 1401–1403 (1979).
30. Penfield, W. & Jasper, H. *Epilepsy And The Functional Anatomy Of The Human Brain* (Little, Brown & Co., Boston, 1954).

Acknowledgements

This work was supported by grants from NIH, the Centre for Consciousness Studies at the University of Arizona and the Keck Foundation. We thank M. Zirlinger for discussions, T. Fields, C. Wilson, E. Isham and E. Behnke for help with the recordings, F. Crick for comments and I. Wainwright for editorial assistance. We also thank all the patients who participated in these studies.

Correspondence and requests for materials should be addressed to I.F. (e-mail: ifried@mednet.ucla.edu).

Real-time prediction of hand trajectory by ensembles of cortical neurons in primates

Johan Wessberg*, Christopher R. Stambaugh*, Jerald D. Kralik*, Pamela D. Beck*, Mark Laubach*, John K. Chapin†, Jung Kim‡, S. James Biggs‡, Mandayam A. Srinivasan‡ & Miguel A. L. Nicolelis*§‖

** Department of Neurobiology; § Department of Biomedical Engineering; ‖ Department of Psychology-Experimental, Duke University, Durham, North Carolina 27710, USA*
† Department of Physiology and Pharmacology, State University of New York Health Science Center, Brooklyn, New York 11203, USA
‡ Laboratory for Human and Machine Haptics, Department of Mechanical Engineering and Research Laboratory of Electronics, MIT, Cambridge, Massachusetts 02139, USA

Signals derived from the rat motor cortex can be used for controlling one-dimensional movements of a robot arm[1]. It remains unknown, however, whether real-time processing of cortical signals can be employed to reproduce, in a robotic device, the kind of complex arm movements used by primates to reach objects in space. Here we recorded the simultaneous activity of large populations of neurons, distributed in the premotor, primary motor and posterior parietal cortical areas, as non-human primates performed two distinct motor tasks. Accurate real-time predictions of one- and three-dimensional arm movement trajectories were obtained by applying both linear and nonlinear algorithms to cortical neuronal ensemble activity recorded from each animal. In addition, cortically derived signals were successfully used for real-time control of robotic devices, both locally and through the Internet. These results suggest that long-term control of complex prosthetic robot arm movements can be achieved by simple real-time transformations of neuronal population signals derived from multiple cortical areas in primates.

Several interconnected cortical areas in the frontal and parietal lobes are involved in the selection of motor commands for producing reaching movements in primates[2–8]. The involvement of these areas in many aspects of motor control has been documented extensively by serial single-neuron recordings of primate behaviour[2,3,8,9], and evidence for distributed representations of motor information has been found in most of these studies[10–13], but little is known about how these cortical areas collectively influence the generation of arm movements in real time. The advent of multi-site neural ensemble recordings in primates[14] has allowed simultaneous monitoring of the activity of large populations of neurons, distributed across multiple cortical areas, as animals are trained in motor tasks[15]. Here we used this technique to investigate whether real-time transformations of signals generated by populations of single cortical neurons can be used to mimic in a robotic device the complex arm movements used by primates to reach for objects in space.

Microwire arrays were implanted in multiple cortical areas of two owl monkeys (*Aotus trivirgatus*)[14–16]. In the first monkey, 96 microwires were implanted in the left dorsal premotor cortex (PMd, 16 wires), left primary motor cortex (MI, 16 wires)[17,18], left posterior parietal cortex (PP, 16 wires), right PMd and MI (32 wires), and right PP cortex (16 wires). In the second monkey, 32 microwires were implanted in the left PMd (16 wires) and in the left MI (16 wires). Recordings of cortical neural ensembles began 1–2 weeks after the implantation surgery and continued for 12 months in monkey 1, and 24 months in monkey 2. During this period, the monkeys were trained in two distinct motor tasks. In task 1, animals